1   Pre-print.

2   El artículo fue aceptado para publicación y fue publicado

3   Editorial: Wiley Online Library

4   DOI: https://doi.org/10.1002/jsfa.9307

5   Rodríguez-López, M.I., Mercader-Ros, M.T., López-Miranda, S., Pellicer, J.A., Pérez-

6   Garrido, A., Pérez-Sánchez, H., Núñez-Delicado, E., Gabaldón, J.A. (2019). Thorough

7   characterization and stability of HP-β-cyclodextrin thymol inclusion complexes prepared

8   by microwave technology: A required approach to a successful application in

9   food. Journal of the Science of Food and Agriculture Disponible. Agriculture 99 (3),

10   1322-1333.

11

12

13

14

15

16

17

18

19

20

21

22

23

Thorough characterization of HP-β-Cyclodextrin Thymol inclusion complexes. A required approach to a successful application in food industry

Running Tittle: Characterization of HP-β-Cyclodextrin Thymol inclusion complexes

Isabel Rodríguez-López[1], Teresa Mercader-Ros[1], Santiago López-Miranda[1], José Antonio Pellicer[1], Alfonso Pérez-Garrido[2], Horacio Pérez-Sánchez[2], Estrella Núñez-Delicado[1], José Antonio Gabaldón[1]*

[1] UCAM Universidad Católica de Murcia. Department of Food Technology and Nutrition. Molecular Recognition and Encapsulation Group (REM). Avenida de los Jerónimos s/n. 30107 Guadalupe. Murcia. Spain.

[2] UCAM Universidad Católica de Murcia. Department of Degree in Computer Science. Bioinformatics and High Performance Computing Group (BIO-HPC). Avenida de los Jerónimos s/n. 30107 Guadalupe. Murcia. Spain.

*Corresponding author: José Antonio Gabaldón Hernández

Telf: +34 968 278622

e-mail: jagabaldon@ucam.edu

UCAM Universidad Católica de Murcia. Department of Food Technology and Nutrition. Avenida de los Jerónimos s/n 30107 Guadalupe, Murcia, Spain.

ABSTRACT

BACKGROUND

The aim of the present study was to obtain a stable dry powder formulation of cyclodextrins (CDs) encapsulating thymol, for a successful application as an ingredient at industrial scale, as well as, to characterize the thymol-CDs complexes by different techniques.

RESULTS

Thymol was successfully solubilized in aqueous solutions and the Kc value increased with the pH of the media until neutral pH, obtaining the highest values (2583 ± 176 L mol^{-1}) for HP-β-cyclodextrins (HP-β-CDs). The best encapsulation efficiency of thymol in solid complexes was obtained using the microwave (MWI) encapsulation method. The different characterization techniques have demonstrated the affinity of HP-β-CDs to thymol molecules, forming stable complexes.

CONCLUSIONS

The results obtained support the use of the MWI method in the preparation of solid HP-β-CD-thymol complexes, due to the greater encapsulation efficiency and technological and economic advantages for industrial applications.

Keywords

Encapsulation, Thymol, HP-β-CDs, spray-drying, microwave irradiation.

INTRODUCTION

73

74   Essential oils (EOs) are volatile and un-colored fluids, easily soluble in lipids and

75   organic solvents. These EOs can be obtained from different plant organs such as roots,

76   flowers, stems or leaves, and their components are usually located in secretory and

77   epidermic cells or glandular trichomes.[1] EOs have a complex composition, containing

78   between 20–60 components at quite different concentrations. Two or three compounds

79   are major components at fairly high concentrations compared to others present in trace

80   amounts.[2] Thymol (2-isopropyl-5-methylphenol), is the major component of the

81   *Origanum* and thyme essential oils, and is the responsible for relevant biological

82   properties of these EOs. In fact, despite having recently received a growing attention as

83   natural biocides, due to their potent activity against a broad range of natural spoilage

84   bacteria, fungi and foodborne pathogens, we found in the literature numerous works

85   focused on the demonstration of their health benefits as antimutagenic, anticancer,

86   antiviral, anti-oxidant, anti-diabetic and anti-inflammatory.[3-10] These properties are due

87   to the presence of their major components, which have a low molecular weight and a high

88   volatility.

89   Thymol is the most abundant compound of the essential oils from plants belonging

90   to the *Lamiaceae* family.[11-13] It has been demonstrated that this phenol has a remarkable

91   antioxidant and anti-inflammatory activity and it is sometimes prescribed as a local

92   anesthetic, contraceptive, healing and antiseptic. In addition, it has antibacterial and

93   antifungal activity, as well as beneficial effects on the cardiovascular system.[14] Different

94   mechanisms of action by which thymol exerts protective effects against cancer have been

95   proposed, as it is able to inhibit cell growth,[15] induce independent and caspase-dependent

96   apoptosis,[16-18] and also the depolarization of mitochondrial membrane.[19]

97   Given the benefits described for thymol in different sectors such as food or

98   agriculture, as well as medicine or pharmacy, it would be interesting developing strategies

99   allowing to solve the drawbacks derived from its physicochemical properties, which

100   restrict its widespread use, such as its low aqueous solubility, its relatively high flavor

101   impact and instability to different environmental factors such as temperature, light and

102   oxygen.

103   In order to solve these drawbacks, the use of different encapsulation techniques has

104   been proposed. Thus, several articles in the literature have focused on the employ of

105   encapsulation technologies for EOs or different components of EOs, including molecular

106   inclusion with host molecules, such as starch,[20] arabic gum,[21] cellulose and polyvinyl-

107   pyrrolidone,[22] chitosan and angicgum,[23-24] liposomes[25-26] and cyclodextrins.[27]

108   Despite that several studies attempted to preserve thymol by cyclodextrins, usually

109   only the formation constant (Kc) of the inclusion complexes has been reported, since

110   complexation was a previous step to achieve another main goal, the experimental

111   evidence of a relevant thymol property.[18,22,24] In this sense, information on different

112   encapsulation methods to maximize thymol concentration in the complex and its stability

113   over time is scarce.

114   Thus, for a successful application as ingredient at industrial scale, producing a

115   standardized dry powder formulation of cyclodextrins encapsulating a volatile and poorly

116   water-soluble molecule is a key challenge, since thymol can leak out during spray drying

117   or storage steps. To the best of our knowledge, this approach has not been yet

118   investigated.

119   Therefore, the present study aimed to optimize a basic work methodology for

120   standardization of the encapsulation process with different CDs types, selecting thymol

121   as model compound, as well as a thorough characterization of the solid complexes by

122 ^{1}HNMR, Fourier transform infrared spectroscopy (FT-IR) and differential scanning

123 calorimetry (DSC) techniques, to evidence the inclusion of thymol into the CDs

124 hydrophobic cavity. In addition, the strength of interactions, geometry, structural aspects

125 and energetically favorable conformation for inclusion complexes formation by applying

126 scanning electron microscopy (SEM) and molecular docking were explored.

127

128   **EXPERIMENTALS**

129 **Reagents and standards**

130   Thymol (99 % purity) was purchased from Sigma (Madrid, Spain). The α- β- and

131 HP-β-CDs were supplied by AraChem (Eindhoven, Holland). Others chemical reagents

132 used were of analytical grade.

133

134 **Solubility studies**

135   The complexation process of thymol in CDs was evaluated by developing phase

136 solubility diagrams, according to the method described by Higuchi and Connors, with

137 some modifications.[28] Excess amounts of thymol were added to 5 mL of aqueous

138 solutions of increasing concentrations of CDs from 0 to 10 mmol L^{-1} for β-CDs, 0 to 50

139 mmol L^{-1} for α-CDs and 0 to 100 mmol L^{-1} for HP-β-CDs. The different phase solubility

140 diagrams were prepared in glass test tubes and maintained in an ultrasonic bath (Ultrasons

141 H.P., Selecta, Spain) for 60 min and 25 ºC, to reach equilibrium.

142   The effect of pH on the complexation process was studied by developing solubility

143 diagrams in buffer solutions of CDs at pH 3.5, 5.5 (sodium acetate buffer 100 mmol L^{-1}),

144 6.5, 7.0 (sodium phosphate buffer mmol L^{-1}) and pH 8.5 (sodium borate buffer 100 mmol

145 L^{-1}).

After 60 min in ultrasound bath, solutions were filtered using 0.45 μm nylon membrane filters to eliminate thymol excess (Chromafil, Macherey-Nagel, Germany). Prior to quantification by GC-MS of thymol content of the complexes in filtered solutions, they were diluted in ethanol (solution:Ethanol, 20:80,v:v). Phase solubility diagrams were carried out in triplicate.

Complexation by using microway as energy source (MWI)

Complexes between HP-β-CDs and thymol were formed by using MWI, as described by Hernández-Sánchez.[29] Solutions of HP-β-CDs (100 mL, from 0 to 100 mmol L^{-1}) were irradiated in a microwave oven (LG Grill Wavedom, LG Electronics Las Rozas, Spain), at 700 W for 30 s at 10 s intervals to reach 70 ºC. Excess of thymol was then added to the HP-β-CDs solutions, which were irradiated again for 30 s at 10 s intervals to reach 70 ºC. Then, the samples were stirred and kept overnight in sealed vials in darkness, at 25 ºC, before being divided in two groups. The first one was filtered using 0.45 μm nylon membrane filters (Chromafil, Macherey-Nagel, Germany) (24h MWI), while the second group was subjected again to the same process 12 hours later (MWI up to 70 ºC, 12 h in darkness and filtration) (48 h MWI). Prior to quantification of thymol content of the filtered samples by GC-MS, they were diluted in ethanol (solution:Ethanol, 20:80,v:v). Phase solubility diagrams were made in triplicate.

Quantification of thymol by GC-MS analysis

The quantification of thymol was carried out by GC-MS analysis. A Shimadzu GC-QP 2010 (Kyoto, Japan) gas chromatographer was used. The GC was combined with a mass spectrometer. Helium was used as carrier gas, at a flow rate of 0.5 mL min^{-1}. A ω-WAX 250 fused silica supelco column (30 m x 0.25 mm x 0.25 μm thickness), was used.

171   The conditions of temperature were as follows: initial temperature at 70 ºC, raised to 160

172   ºC at 4 ºCmin^{-1}, raised to 280 ºC at 30 ºCmin^{-1}, and maintained finally at 280 ºC for 6

173   min. Injector temperature was 250 ºC and injector mode was Split 1:20.

174   The peak area of each sample was used for thymol quantification (mmol L^{-1}), by

175   interpolating in the calibration curve obtained using a standard of thymol, defined by

176   equation: Area = 7544.4+1.80·10^6 [thymol (mmolL^{-1})] and (R^2 = 0.9968) for thymol

177   concentration from 0 to 0.5 mmol L^{-1}.

178

179   **Complexation constant calculation (k$_C$) and complexation efficiency (CE)**

180   Kc between thymol and CDs was calculated from the slope of the phase solubility

181   profile and the solubility of thymol in aqueous solution (S$_0$) by using the equation (1):

182
$$K_C (L{\cdot}mol^{-1}) = \frac{slope}{S_o{\cdot}(1-slope)} \qquad (1)$$

183   CE is the ratio between dissolved complex and free CDs concentration. It is

184   independent of S$_0$, and was calculated from the slope of the phase solubility profiles by

185   using the equation (2).

186
$$CE(\%) = \frac{[disolved-complex]}{[CD]_f} = S_0 * K_C * 100 \qquad (2)$$

187   The molar ratio thymol:CD, was calculated using CE values with equation (3).

188
$$thymol{:}CD = \frac{1}{\left(1+\frac{1}{CE}\right)} \qquad (3)$$

189

190   **Spray dry and stability of dehydrated complexes**

191   The HP-β-CD-thymol solid complexes were obtained by spray dry. The spray

192   dryer used was a Buchi B-290 device (Flawil, Switzerland). The functional parameters of

193   the spray drier were as follows: inlet air temperature 170 ºC, outlet air temperature 68 ºC,

194   35 m^3 h^{-1} of inlet air flow, 5 mL $min^{-1}$of pump flow and 360 L h^{-1} of compressed air

195   caudal. The recovered powder was stored in an airtight glass container prior to

196   analysis.The solid complexes were stored in airtight sealed glass tubes at 25 ºC and 4 ºC.

197   The drying process yield was calculated using equation (4):

198         $$Drying process yield = \frac{\text{dehydrated complexes obtained (g)}}{\text{total solids in solution (kg)}} \qquad (4)$$

199   The encapsulation yield was calculated using equation (5):

200         $$Thymol\ yield = \frac{\text{total thymol in dehydrated complexes (g)}}{\text{total thymol in disolved complexes (kg)}} \qquad (5)$$

201   Prior to quantification of thymol content in the dehydrated complexes by GC-MS,

202   solid complexes were diluted in water (Complex:Water, 1:1,w:v) and filtered using 0.45

203   µm nylon membrane filters (Chromafil, Macherey-Nagel, Germany). Then, dissolved

204   complexes were diluted in ethanol (Complex:Ethanol, 20:80,v:v). Quantification of

205   thymol content in dehydrated complexes was made in triplicate.

206   The stability of the of dehydrated HP-β-CD-thymol complexes was studied by

207   measuring the thymol content in the dehydrated samples during 17 months, maintained

208   at two different temperatures,4 ºC and 25 ºC. Samples were analyzed by triplicate.

209

210   ^{1}H and 2D NMR spectroscopy

211   H-NMR spectra of thymol, CDs, and the inclusion complexes (dissolved in D_2O)

212   were recorded on a 600 MHz spectrometer (Bruker Avance, Germany) at 25 °C. Chemical

213   shifts given in parts per million (ppm), are relative to a tetramethyl silane internal standard

214   (δ=0.0), and NMR data were processed with MestReNova software (6.0.2-5475 version).

215   Two dimensional rotational frame nuclear Overhauser effect spectroscopy (2D ROESY)

216   spectra using the standard Bruker pulse program roesygpph were acquired at 32 scans, an

217   acquisition time of 0.150 s and a pulse delay of 2.3 s.

218

Fourier transform infrared spectroscopy (FT-IR)

219

220   The Fourier transform infrared spectroscopy (FTIR) spectra used to study changes

221 of chemical structures of free thymol, and thymol complex were acquired using a Varian

222 FT-IR 670 (Agilent Tech., the Netherlands) spectrophotometer coupled with an accessory

223 to analyze the attenuated total reflectance (ATR) with a wave number resolution of 0.10

224 cm^{-1} in the range of 250–4,000 cm^{-1}. A minimum of 32 scans were signal-averaged with

225 a resolution of 4 cm^{-1} in the above ranges.

226

Thermal analyses

227

228   The thermal transitions of the isolated and complexed components were recorded

229 by differential scanning calorimetry (DSC), using an analyzer Mettler DSC Q100 (TA

230 Instrument, Cerdanyola del Valles, Spain). Samples of thymol, HP- β-CDs, and thymol

231 complexes were weighed to the nearest 0.1 mg into aluminium capsule and sealed. For

232 the performance of the test, 4-5 mg of sample were weighed into aluminum capsules,

233 which were taken to Hi-Res TGA 2950 thermogravimetric analysis equipment (TA

234 Instrument, Cerdanyola del Valles, Spain), that operated with a scanning rate of 10 °C

235 min^{-1} from 25 ºC to a maximum temperature of 300 °C with nitrogen as the carrier gas.

236 Thermal stability of the respective components is shown using first derivative plots

237 (DTG) of weight (%) against temperature (°C).

238

Field Emission Scanning Electron Microscope (FESEM) images

239

240   The solid complexes were examined under Field Emission Scanning Electron

241 Microscopy (FESEM) using MERLIN™ VP COMPACT (Carl Zeiss Microscopy SL,

242 Germany). The microscopy images were taken using a SE2 detector under an accelerating

243 voltage of 1 kV.

Molecular docking

244

245   The molecular structures for thymol and CDs used in this study were built

246   manually using AutoDockTools[30] and structural information derived from experimental

247   data. The structure of β-CDs was extracted from the crystal structure of the Protein Data

248   Bank (PDB) with code 3CGT. The structure of HP-β-CDs model was built by adding

249   hydroxylpropyl groups to the β-CDs model. Molecular docking calculations were carried

250   out using default parameters in AutoDockVina.[31] Hydroxylpropyl groups of HP-β-CDs

251   were explicitly considered as flexible during docking simulations. Graphical

252   representations of the docking results were prepared using PyMOL (Molecular Graphics

253   System, version 1.3, Schrödinger, LLC).

254

Statistical analysis

255

256   Data were analysed by using the statistical analysis software SPSS (v.21). Values

257   represent means of triplicate determinations and error bars in figures represent standard

258   deviation.

259

RESULTS AND DISCUSSION

260

Complexation of thymol in CDs

261

262   In order to study the ability of CDs to increase the aqueous solubility of thymol,

263   phase solubility studies were carried out at different pHs (3.5; 5.5; 6.5; 7.0; 8.5) at 25 ºC

264   with different types of native or modified CDs (α-CDs; β-CDs; HP-β-CDs). The results

265   obtained by using these types of CDs are shown in Figure 1.

266   The phase solubility diagrams of thymol and CDs showed a linear relationship

267   between thymol and CDs concentration, showing A_L type phase solubility diagrams,

268   which means that the stoichiometry of the inclusion complexes formed were 1:1, in all

269   cases.

270   Assuming the formation of 1:1 complexes, it was possible to calculate the

271   complexation constant (Kc) and the complexation efficiency (CE) values between thymol

272   and CDs, by using linear regression analysis ofthe phase solubility diagrams according to

273   equations 1 and 2. The Kc value describes the strength of the interaction between thymol

274   and CDs, and can be used to compare the stability of the complexes formed between

275   thymol and each type of CDs. The solubilising effect of CDs is showed by the

276   complexation efficiency (CE). This parameter is independent on S_0,[32] and represents the

277   molar ratio between complex and free CDs concentration.[33] The values of S_0, Kc and CE

278   are shown in Table 1.

279   The experimental data showed that the Kc value increased with pH until neutral

280   pH. This effect could be due to the fact that the solubility (S_0) of thymol decreased from

281   6.42 mmol L^{-1} to 5.54 mmol L^{-1} as pH increased from 3.5 to 7.0. However, a slight

282   increase at pH 8.5 (5.92 mmol L^{-1}) was observed. It should be noted that the aromatic

283   structure of thymol (derived from phenol), determines its reactivity, behaving as a weak

284   acid (pKa = 10.62). Therefore, the pH of the medium could conditionits dissociation

285   degree and consequently its solubility.

286   Being more acidic than water and coming into contact with alkaline hydroxides in

287   aqueous solution at basic pH, thymol reacts with alkaline hydroxides to form salts or

288   phenoxide ions, more stable than thymol itself (at neutral pH), due to the net effect of the

289   resonance of the aromatic ring. The formation of thymol inclusion complexes with CDs

290   determines a decrease in the enthalpy and an increase in the entropy of the system,

291   reducing thus the free energy, which causes an increase in the stability of the complex.

292   Therefore, the protonation of thymol and its solubility are determinants in the complexes

12

293   stability. Taken into account that the internal cavity of the CD is quite hydrophobic, the

294   inclusion of apolar and uncharged species is favored versus polar hydrated or net charge

295   species, since the inner surface of the cone that will receive the host molecule is apolar.

296   In fact, for the three types of CDs studied (Table 1), a significant increase in complexes

297   stability (Kc values) at pH 7 was observed.

298   In relation to CDs cavity size, the Kc values obtained for native CDs were higher

299   for β- than for α–CDs (Table 1). The size of the hydrophobic cavity of α-CDs (0.49 nm)

300   may be too small, whereas β-CDs (0.62 nm), is more appropriate to accommodate therein

301   the aromatic rings of thymol (Figure 1).

302   With respect to the Kc values, differences observed between β- and HP-β-CDs

303    $(1184 \pm 115$ L mol^{-1}and 2583 ± 176L mol^{-1}, respectively), these could be due to the

304   intensity of the hydrophobic forces and van der Waals interactions involved, the release

305   of the ring stress, and to a greater extent, the presence of hydroxypropyl groups in the

306   modified CDs, making the thymol molecules more accessible to the apolar cavity. On the

307   other hand, the hydroxypropyl groups may also cause the opening of the CD cavity,

308   significantly modifying its size with respect to the native CD, thereby favoring the

309   complete thymol molecule inclusion in the internal cavity of the HP-β-CDs, whereas in

310   the case of β-CDs, is only able to penetrate a part of the thymol molecule.

311   However, it is important to note that the value of Kc does not depend only on the

312   increase in the aqueous solubility of thymol when complexed with CDs, but also on the

313   aqueous solubility (S_0) of thymol. Therefore, the efficacy of thymol complexation (CE)

314   and the molar ratio (thymol:CD) for each type of CDs (Table 1), were also determined by

315   using equations (2) and (3).

316   The comparison of CE parameter is more convenient than comparing Kc values

317   when the study involves different types of CDs, or different complexation conditions for

318 the same compound. CE values obtained ranged from 37.8% for α-CDs at pH 7.0 to

319 139.5% for HP-β-CDs at pH 7.0 (Table 1). This high value above 100% indicates that at

320 pH 7.0, there are more HP-β-CDs complexing thymol than free in solution. The values

321 obtained for molar ratio ranged from 1:4 to 1:2, indicating that about one of every 4 or 2

322 CDs molecules in solution is forming soluble complexes whit thymol (Table 1).

323 Comparing the tree types of CDs studied, α-CDs showed lowest CE values and

324 molar ratio (between 1:4 and 1:3) than those obtained for β- or HP-β-CDs. In the case of

325 β- and HP-β-CDs, molar ratio were between 1:3 and 1:2, indicating that in many cases

326 one of every 3 or 2 β- or HP-β-CDs molecules in solution is forming soluble complexes

327 whit thymol.

328 In summary, HP-β-CDs at pH 7.0 showed the highest Kc value (2583 ± 176 L

329 mol^{-1}) and the highest CE (139.5%) for thymol complexation, despite of at this pH,

330 thymol presented its lower aqueous solubility (0.54 ± 11 mmol L^{-1}) (Table 1).

331

332 **Complexes formation optimization**

333 Once the ability of α-, β- and HP-β-CDs to form inclusion complexes with thymol

334 has been demonstrated, HP-β-CDs were selected to optimize the complexes formation

335 because of their higher CE (139.5±12.3%) and Kc (2583 ± 176L mol^{-1}) values at neutral

336 pH (7.0) with respect to the native CDs tested. To optimize the encapsulation of thymol

337 by HP-β-CDs, two encapsulation methods were compared: solubility and microwave

338 irradiation method (MWI) described by Hernández-Sánchez.[29]

339 Figure 2 shows the phase diagrams obtained using the solubility and microwave

340 irradiation methods. Both methods showed that the stoichiometry of the complexes

341 obtained was 1:1, and no difference between the number of microwave cycles applied to

342 the samples (○ 24 h MWI, ● 48 h MWI) were observed. The Kc values obtained by using

343   one or two microwave cycles were 4835 ± 94 L mol^{-1} and 4696 ± 87 L mol^{-1}, respectively,

344   indicating that a contact time of 24 h and the application of only one microwave cycle

345   were adequate to reach the equilibrium of the mixture. So, the Kc value between thymol

346   and HP-β-CDs used from now on will be the average value 4765 ± 90.5 L mol^{-1}. However,

347   this value of Kc obtained by using MWI method was significantly higher than that

348   obtained by the solubility method (2583 ± 176 L mol^{-1}). This result could be due to the

349   fact that microwave irradiation has the ability to penetrate into any substance, causing the

350   rotation of molecules with an electric dipole such us water molecules. In other words, it

351   stimulates the interaction of some molecules with others, favoring the exit of the water

352   molecules from the CDs cavity, a circumstance that takes advantage for the thymol

353   molecules to enter into the empty apolar cavity.[34]

354   It should be noted that microwave irradiation does not affect the activation energy

355   required to initiate the complexation, but provides almost instantaneously enough energy

356   to overcome this barrier, and complete the reaction more quickly and with greater

357   efficiency than using other methods of energy application. In addition, the energy

358   transmitted by the microwaves affects the temperature parameters described in the

359   Arrhenius equation. As a consequence, this instantaneous heating causes a faster

360   molecular movement (increase of the kinetic energy), generating a greater number of

361   collisions and favoring the dissolution of the different compounds.

362

363 Complexes dehydration and stability

364   Soluble complexes HP-β-CDs-thymol were subjected to a spray drying process to

365   obtain complexes in solid state. This drying method was applied because it is widely used

366   in the food industry, and in addition, there are different studies that corroborate its

367   usefulness in obtaining solid complexes with CDs.[35-37]

368   The structure and size of the solid complexes obtained from the dehydration

369   process were analysed. The analysis of the appearance of the dehydrated structures

370   obtained by scanning electron microscope (SEM) images, showed that the spray dried

371   complexes were composed of irregular particles with spherical shape, revealing numerous

372   folds and dents at the surface (Figure 3 B and C). This geometric shape and variable size

373   is typical of the materials obtained by spraydrying.[38]

374   According to Loksuwan,[39] the folds at the surface of the atomized particles and

375   the expansion of their size, are usually generated as a result of the presence of core

376   materials (CDs), since they slow down the evaporation rate of the system water due to

377   their ability to retain water molecules (Figure 3). As can be seen in Figure 3 (B and C),

378   the outer surfaces of certain complexes show continuous walls, without cracks, which

379   have a significant influence on the retention of volatile compounds.

380   In previous studies some particle morphologies are described, such us

381   microencapsulated coffee oil,[40] oregano essential oil[41] and laurel infusions.[42] In all cases,

382   microparticles with external globular morphology similar to those described in Figure 3

383   were described.

384   The yield of the dry process was also calculated by using Equations 4 and 5, and

385   the results are shown in Figure 4.The drying process yield was higher than 500 g of solid

386   material recuperated by kg of solid material introduced into the spray dryer, but lower

387   than 800 g kg^{-1} in all HP-β-CDs concentration used. At laboratory scale, it is difficult to

388   achieve yields above 800 g kg^{-1},[43] since the quantity of soluble solids are generally small

389   and therefore the proportion of material lost during the drying process is high. At

390   industrial scale, by increasing the working quantities, the drying yield would be higher,

391   with values above 900 g kg^{-1}. The dry process yield (Figure 4A) was dose-dependent,

392   showing higher values as HP-β-CDs concentration increased. The highest dry process

393   yield (766 g kg^{-1}) was obtained for a 100 mmol L^{-1} HP-β-CDs concentration using the

394   solubility method.

395   The dry process yield tended to be higher for the solubility encapsulation method

396   than MWI encapsulation method (Figure 4A). The difference between both methods

397   could be justified considering that for the same CDs concentration; there was a higher

398   quantity of thymol in solution when complexes were formed by MWI, resulting in a

399   higher quantity of solids in the dried mixture, and also increasing the solution viscosity.[38]

400   This fact could provoke a greater adhesion of the dehydrated powder to the wall of the

401   dehydration chamber, increasing the amount of solid complexes lost and reducing the dry

402   process yield.[44]

403   The thymol retention capacity after the dehydration process was evaluated by the

404   thymol yield (Equation 5). The data obtained are shown in Figure 4B. Comparing the

405   thymol yield achieved by drying complexes obtained by both, solubility and MWI

406   methods, it was observed that the values obtained were on average, 28 % higher for the

407   MWI samples. These results could be explained considering that CDs reach an instant

408   state of resonance with the MWI method, and therefore, favoring the exit of water

409   molecules from the CDs cavity, and the input of the thymol molecules.[45]

410

411   **Stability of solid complexes**

412   The stability of solid complexes was also studied, evaluating the content of thymol

413   in the powder with the storage time, at different temperatures. As it is shown in Figure 5,

414   the solid complexes coming from MWI tend to retain more effectively the thymol (Figure

415   5, B). When the storage temperature was 25 °C, the thymol losses at 17 months of storage

416   was 20% in the case of MWI complexes (Figure 5B, ●), whereas it was more than 50%

417   in the case of solubility method complexes (Figure 5A, ●).

418   When the storage temperature was 4 ºC, HP-β-CDs-thymol complexes obtained

419   by MWI were able to avoid the losses of thymol until the fourth month of storage,

420   although from that moment, the losses increased in a significant way reaching a loss

421   percentage of 75% at 17 months. It was also observed that the conservation of the

422   complexes at a low temperature (4 ºC) increased the losses of thymol in a more

423   pronounced way than at 25 ºC. These results can be justified considering that, by storing

424   the samples at a lower temperature, the moisture content in the surrounding environment

425   increases considerably, favoring an unequal competition between the thymol and water

426   molecules for the CDs internal cavity (hygroscopic molecules), causing the release of the

427   thymol complexed.

428   These results agree with those previously described by Mohit,[46] for the

429   complexation of cefdinir with β-CDs by MWI and subsequent atomization.

430

Nuclear magnetic resonance (NMR)

432   ^{1}H NMR spectra of thymol, HP-β-CDs, and the inclusion complexes (dissolved in

433   D_2O) were obtained. Thymol was really included inside the lipophilic HP-β-CDs cavity.

434   Other techniques like DSC, IR, UV-Vis, are able to either suggest or establish if the guest

435   molecules form a complex or not, but they are unable to give any sure finding, neither on

436   the kind of complex (if inclusion or adsorption) nor on the structural conformation of the

437   molecules.[20] Analyzing data obtained from ^{1}H-NMR experiments it was possible to define

438   the stoichiometry of the complexes: for either thymol the ratio was 1:1. Table 2 reportsthe

439   chemical shift values of thymol and HP-β-CDs protons (Figure 1 A-B), in the free and

440   complex state in D_2O solution, as well as the differences between the signals of the free

441   and included molecules.

442   Besides, it is well known that two-dimensional (2D) NMR spectroscopy provides

443   important information about the spatial proximity between host and guest atoms via

444   observation of intermolecular dipolar cross-correlations. Two protons which are closely

445   located in space can produce a nuclear Overhauser effect (NOE) cross-correlation

446   between the relevant protons in NOESY or ROESY spectrum. The presence of NOE

447   cross-peaks between protons from two species indicates spatial contacts within 0.4 nm.

448   In order to gain more conformational information, 2D ROESY of the HP-β-CDs-thymol

449   inclusion complexes was obtained and it is shown in Figure 6.

450   The ROESY spectrum of the HP-β-CDs-thymol complex showed appreciable

451   correlation of the OH proton of thymol with the H-5 protons of HP-β-CDs and the T2"

452   proton of thymol with the H-5 protons of HP-β-CDs (Figure 1 A, B). These results clearly

453   indicate that thymol was included in the HP-β-CDs cavity.

454

Molecular Docking

456   To understand how thymol interacts with HP-β-CDs once complexed, docking

457   simulations were carried out. Additionally, the structural information about the binding

458   pose obtained by docking was shown in Figure 7, where thymol is observed to penetrate

459   into the hydrophobic cavity of HP-β-CDs, detecting strong van der Waals interactions

460   between the atoms of both molecules.

461   Figure 7C represents the view from the top of the complex (conical perspective),

462   where thymol is shown in red, the atoms of the hydroxypropyl group of HP-β-CDs appear

463   in blue, and the remaining atoms of HP-β-CDs are represented in green. The opposite

464   view is shown in Figure 7D, where thymol is shown in red, the atoms of the

465   hydroxypropyl group of HP-β-CDs in blue, and the other atoms of HP-β-CDs in green.

It is observed that thymol binds tightly into HP-β-CDs internal cavity. Hydrogens T2″ from isopropyl group from thymol interact with hydrogen atoms H3 of HP-β-CDs (green sphere in figure 7A), and the hydrogen from hydroxyl group of thymol interacts with the atoms of hydrogen H5 of HP-β-CDs (purple sphere from figure 7A). The carbon atoms of the hydroxypropyl groups of HP-β-CDs are shown in light blue, while the remaining carbon atoms of HP-β-CDs are presented in green color (Figure 7B). These results agree with ¹H 2D-ROESY NMR data obtained (Figure 6). Also, it is clear that with this conformation, thymol binds tightly into HP-β-CDs hydrophobic core, if we have a look at the spheres representation of the molecules as shown in figure 7B, 7C and 7D.

Differential scanning calorimetry (DSC) and thermogravimetric analysis (TG)

Differential scanning calorimetry also was used for the recognition of inclusion complexes. When guest molecules are embedded into CDs cavities, their melting, boiling or sublimating points generally shifted to different temperature or disappeared. DSC and thermogravimetic analysis (TG) curves are shown in Figure 8.

The DSC curves of thymol presented three endothermic bands at about 50, 120 and 165-170 ºC. The first one is associated to its melting point (Figure 8A, a) and the rest which could be due to oxidation and volatilization of the chemical, with a 95% of mass reduction, as can be seen in TG analysis (Figure 8B, c). For HP-β-CDs, owing to its amorphous nature, a broad endothermic peak was observed approximately at 70 °C (Figure 8A, c) associated with its dehydration. An overall reduction of this signal is evident when thymol is complexed with CDs, suggesting a water exclusion process during complex formation (Figure 8A, b). The DSC curve of the HP-β-CDs-thymol complex (Figure 8A, b) did not exhibit the characteristic endothermic peaks of thymol

490 (Figure 8A, a), indicating that this compound was protected due to the formation of the

491 inclusion complex with HP-β-CDs.

492   The TG analysis (Figure 8, B) showed a different percentage of mass loss at 50

493 °C, corresponding mainly to the water embedded into HP-β-CDs. The TG curve of HP-

494 β-CDs presented a weight loss of 5% (Figure 8B, a), and the HP-β-CDs-thymol curve had

495 a weight loss of 2.79% (Figure 8B, b). This situation suggests a water molecules reduction

496 in the internal cavity of HP-β-CDs due to the inclusion of thymol. Similar results were

497 observed in a previous study between thymol and β-CDs.[47]

498

499 **Fourier transform infrared spectroscopy (FT-IR)**

500   FTIR is a useful technique used to confirm the formation of an inclusion

501 complex.[48] The IR spectrum of HP-β-CDs (Figure 9) showed several peaks: 3341 cm^{-1}

502 (O-H stretching vibrations); 2923 cm^{-1}(C-H stretching vibrations); 1643 cm^{-1} (O-H

503 bending vibrations); 1157 cm^{-1}(C-O vibration); 1012 cm^{-1} (C–O–C stretching

504 vibrations); 850 cm^{-1}(α-type glycosidic bond); 2967 cm^{-1} (anti-symmetric vibration of

505 methyl groups); 1375 cm^{-1} (bending vibration of methyl).

506   The IR spectrum of thymol (Figure 9, inset), showed O-H stretching band at 3166

507 cm^{-1}, narrow peak of OH bending in plane at 1457 cm^{-1}, C=C aromatic stretching at 1621

508 cm^{-1}, 1585 cm^{-1}, and 1458 cm^{-1}; stretching C-H aromatic bend out of plane at 736 cm^{-1},

509 CH$_3$ symmetric and asymmetric stretching bands at 2866 and 2958 cm^{-1}, respectively,

510 and 804 cm^{-1} for out-of-plane CH wagging vibrations.The in plane C-H bending was

511 observed at 1089 cm^{-1} and 1058 cm^{-1}.

512   In the Figure 9, it should be noted that the bands of free thymol molecules were

513 generally covered up by the peaks of HP-β-CD-thymol complex because the quantities of

514 the guest molecules were no more than10–15 % (w/w) in the inclusion complexes.[49] The

two band of HP-β-CDs at 2923 and 2967 cm^{-1} corresponding to a C-H stretching vibrations and anti-symmetric vibration of methyl groups, respectively, were slightly shifted to 2925 and 2965 cm^{-1} and they have greater intensity. Moreover, the peak of C=C aromatic stretching of thymol at 1621 cm^{-1} appears in the HP-β-CDs-thymol complex shifted at 1619 cm^{-1}. This slight shifts relative to those of the respective free compounds, providing an evidence of host-guest interactions.

CONCLUSIONS

In conclusion, the results obtained in the stability study support the use of the MWI method in the preparation of solid HP-β-CD-thymol complexes, with a contact time of 24 h, due to the greater efficiency of encapsulation, but also other technological and economic advantages of great interest for industrial applications, such as process escalation at industrial level, or cost reduction (energy and labor saving). Moreover, MWI allows a rapid reaction heating without overheating the product, speeding up the process kinetics. The different characterization techniques have demonstrated the affinity of HP-β-CDs to thymol molecules, forming stable complexes.

REFERENCES

1. Sell C, Chemistry of essential oils, in *Handbook of Essential Oils: Science, Technology and Applications*, ed. by Başer KH and Buchbauer G. CRC Press, Boca Raton (Florida, USA), pp. 121–150 (2010).

2. Bilia AR, Guccione C, Isacchi B, Righeschi C, Firenzuoli F and Bergonzi MC, Essential oils loaded in nano systems: a developing strategy for a successful therapeutic approach. *Evidence-Based Complementary and Alternative Medicine* **651593:**1-14 (2014).

3. Vunda SLL, Sauter IP, Cibulski SP, Roehe PM, Bordignon SAL, Rott MB, Apel MA and von Poser GL, Chemical composition and amoebicidal activity of *Croton pallidulus*, *Croton ericoides*, and *Croton isabelli* (Euphorbiaceae) essential oils. *Parasitol Res* **111:**961–966 (2012).

4. da Cruz L, Pinto VF and Patriarca A, Application of plant derived compounds to control fungal spoilage and mycotoxin production in foods. *Int J Food Microbiol* **166:**1–14 (2013).

5. Elizaquível P, Azizkhani M, Aznar R and Sánchez G, The effect of essential oils on norovirus surrogates. *Food Control* **32:**275–278 (2013).

6. Gautam N, Mantha AK and Mittal S, Essential oils and their constituents as anticancer agents: a mechanistic view. *Bio Med Res Int* **2014:**1-23. (2014).

7. Liju VB, Jeena K and Kuttan R, Chemopreventive activity of turmeric essential oil and possible mechanisms of action. *Asia Pac J Cancer Prev* **15:**6575–6580 (2013).

8. Arranz E, Jaime L, de las Hazas ML, Reglero G and Santoyo S, Supercritical fluid extraction as an alternative process to obtain essential oils with anti-inflammatory properties from marjoram and sweet basil. *Ind Crop Prod* **67:**121–129 (2015).

564 9. Sheikh BA, Pari L, Rathinam A and Chandramohan R, Trans-anethole, a terpenoid

565 ameliorates hyperglycemia by regulating key enzymes of carbohydrate metabolism

566 in streptozotocin induced diabetic rats. *Biochimie* **112:**57–65 (2015).

567 10 Silva F and Domingues FC, Antimicrobial activity of coriander oil and its

568 effectiveness as food preservative. *Crit Rev Food Sci* **57:**35-47 (2015).

569 11. Licata M, Tuttolomondo T, Dugo G, Ruberto G, Leto C, Napoli EM, Rando R, Rita

570 Fede M, Virga G and Leone R, Study of quantitative and qualitative variations in

571 essential oils of Sicilian oregano biotypes. *J Essent Oil Res* **27:**293–306 (2015).

572 12. Mancini E, Senatore F, Del Monte D, De Martino L, Grulova D, Scognamiglio M,

573 Snoussi M and De Feo V, Studies on chemical composition, antimicrobial and

574 antioxidant activities of five *Thymus vulgaris* L. essential oils. *Molecules* **20:**12016–

575 12028 (2015).

576 13. Sarwar A and Latif Z, GC–MS characterisation and antibacterial activity evaluation

577 of Nigella sativa oil against diverse strains of Salmonella. *Nat Prod Res* **29:**447–

578 451 (2015).

579 14. Marchese A, Orhan IE, Daglia M, Barbieri R, Di Lorenzo A, Nabavi SF, Gortzi O,

580 Izadi M and Nabavi SM, Antibacterial and antifungal activities of thymol: A brief

581 review of the literature. *Food Chem* **210:**402–414 (2016).

582 15. Jaafari A, Tilaoui M, Mouse HA, M'bark LA, Aboufatima R, Chait A, Lepoivre M

583 and Zyad A, Comparative study of the antitumor effect of natural monoterpenes:

584 relationship to cell cycle analysis. *Rev Bras Farmacogn* **22:**534–540 (2012).

585 16. Deb DD, Parimala G, Devi SS and Chakraborty T, Effect of thymol on peripheral

586 blood mononuclear cell PBMC and acute promyelotic cancer cell line HL-60.

587 *Chem-bio Interac* **193:**97–106 (2011).

588 17. Yin Q, Yan F, Zu XY, Wu Y, Wu X, Liao M, Deng S, Yin L and Zhuang Y, Anti-
589   proliferative and pro-apoptotic effect of carvacrol on human hepatocellular
590   carcinoma cell line HepG-2. *Cytotechnology* **64:**43–51 (2012).

591 18. Llana-Ruiz-Cabello M, Gutiérrez-Praena D, Puerto M, Pichardo S, Jos Á and
592   Cameán AM, In vitro pro-oxidant/antioxidant role of carvacrol, thymol and their
593   mixture in the intestinal Caco-2 cell line. *Toxicol in Vitro* **29:**647–656 (2015).

594 19. Lai WW, Yang JS, Lai KC, Kuo CL, Hsu CK, Wang CK, Chang CY, Lin JJ, Tang
595   NY and Chen PY, Rhein induced apoptosis through the endoplasmic reticulum
596   stress, caspase-and mitochondria- dependent pathways in SCC-4 human tongue
597   squamous cancer cells. *In Vivo* **23:**309–316 (2009).

598 20. Marques HM, A review on cyclodextrin encapsulation of essential oils and
599   volatiles. *Flavour Frag J* **25:**313–326 (2010).

600 21. Ponce-Cevallos PA, Buera MP and Elizalde BE, Encapsulation of cinnamon and
601   thyme essential oils components (cinnamaldehyde and thymol) in β-cyclodextrin:
602   effect of interactions with water on complex stability. *J Food Eng* **99:**70–75 (2010).

603 22. Nieddua M, Rassua G, Boattoa G, Bosib P, Trevisib P, Giunchedia P, Cartaa A and
604   Gavini E, Improvement of thymol properties by complexation with cyclodextrins:
605   In vitro and in vivo studies. *Carbohyd Polym* **102:**393–399 (2014).

606 23. Glenn GM, Klamczynski AP, Imam SH, Chiou B, Orts WJ and Woods DF,
607   Encapsulation of plant oils in porous starch microspheres. *J Agric Food Chem*
608   **58:**4180–4184 (2010).

609 24. Guarda A, Rubilar JF, Miltz J and Galotto MJ, The antimicrobial activity of
610   microencapsulated thymol and carvacrol. *Int J Food Microbiol* **146:**144–150
611   (2011).

612   25. Meunier JP, Cardot JM, Gauthier P, Beyssac E and Alric M, Use of rotary

613   fluidized-bed technology for development of sustained-release plant extracts

614   pellets: Potential application for feed additive delivery. *J Anim Sci* **84:**1850–1859

615   (2006).

616   26. Higueras L, López-Carballo G, Cerisuelo JP, Gavara R and Hernández-Muñoz P,

617   Preparation and characterization of chitosan/HP-β-cyclodextrins composites with

618   high sorption capacity for carvacrol. *Carbohyd Polym* **97:**262–268 (2013).

619   27. Del Toro-Sánchez C, Ayala-Zavala J, Machi L, Santacruz H, Villegas-Ochoa M,

620   Alvarez-Parrilla E and González-Aguilar G, Controlled release of antifungal

621   volatiles of thyme essential oil from β-cyclodextrin capsules. *J Incl Phenom Macro*

622   **67:**431–441 (2010).

623   28. Higuchi T and Connors KA, Phase solubility techniques. *Adv Anal Chem Instrum*

624   **4:**56-63 (1965).

625   29. Hernández-Sánchez P, López-Miranda S, Guardiola L, Serrano-Martínez A,

626   Gabaldón JA and Nuñez-Delicado E, Optimization of a method for preparing solid

627   complexes of essential clove oil with β-cyclodextrins. *J Sci Food Agr* **97:**420-426

628   (2017).

629   30. Morris GM, Huey R, Lindstrom W, Sanner MF, Belew RK, Goodsell DS and Olson

630   AJ, AutoDock4 and AutoDockTools4: Automated docking with selective receptor

631   flexibility. *J Comput Chem* **30:**2785−2791 (2009).

632   31. Trott O and Olson AJ, Auto Dock Vina: Improving the speed and accuracy of

633   docking with a new scoring function, efficient optimization, and multithreading. *J*

634   *Comput Chem* **31:**455− 461 (2010).

635 32. Li R, Quan P, Liu D, Wei F, Zhang Q and Xu Q, The influence of co-solvent on

636   the complexation of HP-β-cyclodextrins with oleanolic acid and ursolic acid. *AAPS*

637   *Pharm Sci Tech* **10:**1137-1144 (2009).

638 33. Loftsson T and Hreinsdóttir D, The complexation efficiency. *J Incl Phenom Macro*

639   **57:** 545-552 (2007).

640 34 Kappe CO, Controlled microwave heating in modern organic synthesis. *Angew*

641   *Chem Int Ed* **43:**6250–6284 (2004).

642 35. Reineccius TA, Reineccius GA and Peppard TL, Encapsulation of flavors using

643   cyclodextrins: comparison of flavor retention in alpha, beta, and gamma types. *J*

644   *Food Sci* **67:**3271–3279 (2002).

645 36. Jaafari SM, Assadpoor E, He Y and Bhandari B, Encapsulation efficiency of food

646   flavours and oils during spray drying. *Dry Technol* **26:**816–835 (2008).

647 37. Wu Y, Zou L, Mao J, Huang J and Liu S, Stability and encapsulation efficiency of

648   sulforaphane microencapsulated by spray drying. *Carbohyd Polym* **102:**497–503

649   (2014).

650 38. Fernandes RV, Borges SV and Botrel DA, Gum arabic/starch/maltodextrin/inulin

651   as wall materials on the microencapsulation of rosemary essential oil. *Carbohyd*

652   *Polym* **101:**524–532 (2014).

653 39. Loksuwan J, Characteristics of microencapsulated β-carotene formed by spray

654   drying with modified tapioca starch, native tapioca starch and maltodextrin. *Food*

655   *Hydrocolloid* **21:**928–935 (2007).

656 40. Frascareli EC, Silva VM, Tonon RV and Hubinger MD, Effect of process

657   conditions on the microencapsulation of coffee oil by spray drying. *Food Bioprod*

658   *Process* **90:**413–424 (2012).

659   41. Alvarenga D, Vilela S, Fernandes R, Viana A, Gomes J and Marques G, Evaluation

660   of spray drying conditions on properties of microencapsulated oregano essential oil.

661   *Int J Food Sci Technol* **47:**2289–2296 (2012).

662   42. Medina-Torres L, Santiago-Adame R, Calderas F, Gallegos-Infante JA, González-

663   Laredo RF, Rocha-Guzmán NE, Núñez-Ramírez DM, Bernad-Bernad MJ and

664   Manero O, Microencapsulation by spray drying of laurel infusions

665   (*Litseaglaucescens*) with maltodextrin. *Ind Crop Prod* **90:**1–8 (2016).

666   43. Arpagaus C and Schafroth N, Spray drying of biodegradable polymers in laboratory

667   scale. *Resp Drug Deliv Eur* **2009:**269–74 (2009).

668   44. Tonon RV, Brabet C and Hubinger MD, Influence of process conditions on the

669   physicochemical properties of açai (*Euterpe oleraceae* Mart.) powder produced by

670   spray drying. *J Food Eng* **88:**411– 418 (2008).

671   45. Bergese P, Colombo I, Gervasoni D and Depero LE, Microwave generated

672   nanocomposites for making insoluble drugs soluble. *Mat Sci Eng C* **23:**791–795

673   (2003).

674   46. Mohit V, Harshal G, Neha D, Vilasrao K and Rajashree H, A comparative study of

675   complexation methods for cefdinir-hydroxypropyl-β-cyclodextrinsystem. *J Incl*

676   *Phenom Macro* **71:**57–66 (2011).

677   47. Fernandes LP, Éhen Z, Moura TF, Novák C and Sztatisz J, Characterization of

678   lippies idoides oil extract β-cyclodextrin complexes using combined

679   thermoanalytical techniques. *J Thermal Anal Calorim* **78:**557–573 (2004).

680   48. Ahmed SM, Naggi A, Guerrini M and Focher B, Inclusion complexes of

681   bropirimine with b-cyclodextrin in solution and in solid state. *Int J Pharmaceut*

682   **77:**247–254 (1991).

683   49. Yang Y and Song LX, Study on the inclusion compounds of eugenol with α-, β-,

684   γ- and Heptakis (2, 6-di-O-methyl)-β-cyclodextrins. *J Incl Phenom Macro* **53:**27–

685   33 (2005).

686

687

688

689

690

691

692

693

694

695

696

697

698

699

700

701

702

703

704

705

706

707　　Table 1. Aqueous solubility (S_0), complexation constant (Kc), correlation coefficient of

708　　the phase solubility diagram (r^2), complexation efficiency (CE) and molar ratio of thymol

709　　for α-, β- and HP-β-CDsat different pH. ±SD. Standard deviation of triplicate diagrams.

	pH	S_0 (mmol L^{-1})	Kc (L mol^{-1})	r^2	CE (%)	Molar ratio
α-CD	3.5	6.42±0.20	281±26	0.971	39.9±5.0	1:4
	5.5	6.19±0.15	336±22	0.998	40.0±4.0	1:4
	6.5	6.02±0.12	600±54	0.991	61.2±10.1	1:3
	7.0	5.54±0.11	701±90	0.992	37.8±5.2	1:4
	8.5	5.92±0.10	592±97	0.993	54.5±0.12	1:3
β-CD	3.5	6.42±0.20	701±39	0.960	79.0±11.0	1:2
	5.5	6.19±0.15	866±19	0.944	71.9±13.0	1:2
	6.5	6.02±0.12	913±80	0.987	67.7±12.0	1:2
	7.0	5.54±0.11	1184±115	0.988	63.9±10.6	1:3
	8.5	5.92±0.10	580±45	0.988	53.3±9.1	1:3
HP-β-CD	3.5	6.42±0.20	291±19	0.988	41.3±6.0	1:3
	5.5	6.19±0.15	493±37	0.987	58.6±7.0	1:3
	6.5	6.02±0.12	638±73	0.997	65.0±5.0	1:3
	7.0	5.54±0.11	2583±176	0.999	139.5±12.3	1:2
	8.5	5.92±0.10	778±64	0.994	71.6±8.0	1:2

710

711

712

713

714

715

716

717

718

719

720   Table 2. ^{1}H-NMR Chemical Shifts (δ) of thymoland HP-β-CD, in the free and complexed

721   forms, in D₂O.

	H-Atom	δ ppm⁻¹ (Free)	δ ppm⁻¹ (Complexed)	Δδ (Complexed - Free) ppm⁻¹
Thymol	H-C (3)	6.967	6.968	-0.001
	H-C (4)	6.573	6.575	-0.002
	H-C (6)	6.560	6.551	0.009
	H-C (2')	3.265	3.274	-0.009
	H-C (5')	2.197	2.202	-0.005
	H-C (2")	1.169	1.172	-0.003
HP-β-CD	H-C (1)	5.074	5.070	0.004
	H-C (2)	3.723	3.726	-0.003
	H-C (3)	3.947	3.945	0.002
	H-C (4)	3.418	3.416	0.002
	H-C (5)	3.534	3.532	0.002
	H-C (6)	3.821	3.817	0.004
	H-C (9)	1.126	1.125	0.001

722

723   *Molecular structure and atom numbering for thymol and HP-β-CD monomer are depicted in Figure 1 (A-B).*

724

725

726

727

728

729

730

731

732

733
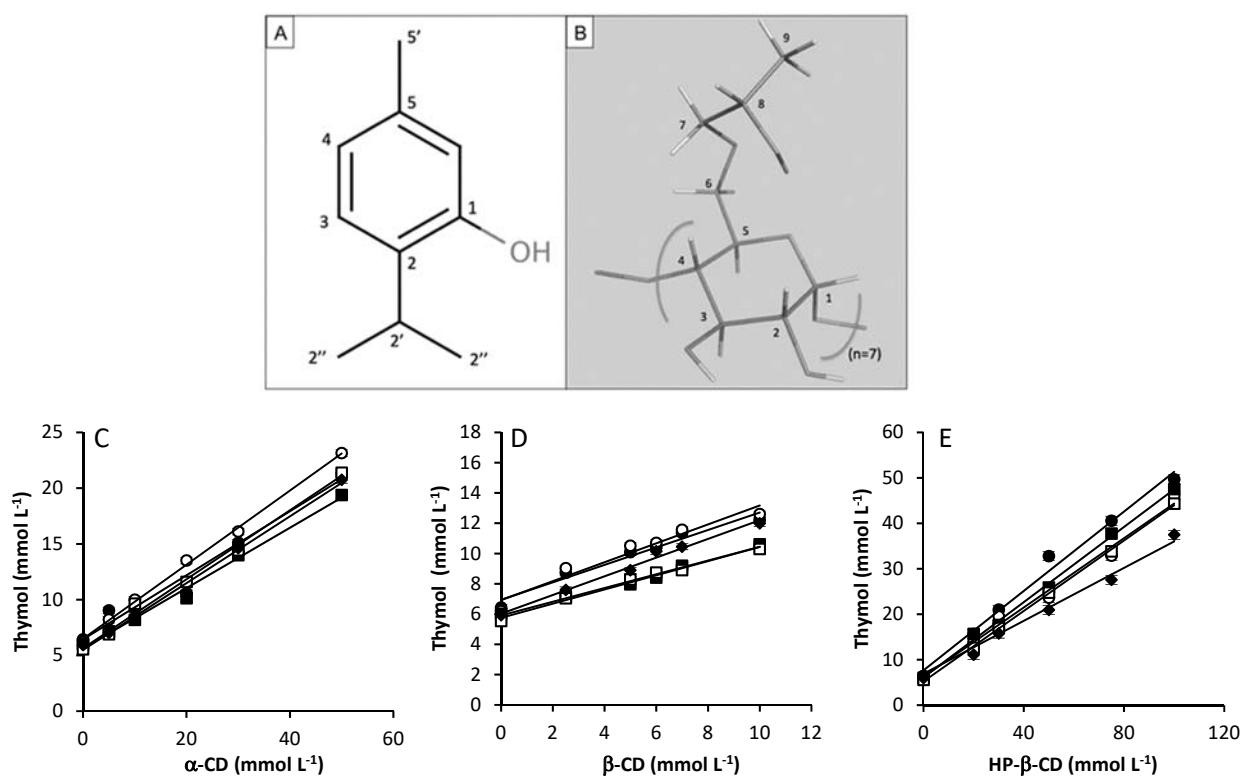
Figure 1. Molecular structure and atom numbering for thymol(A) and HP-β-CD monomer (B). Phase solubility diagrams of thymol with α-CDs (C), β-CDs (D) and HP-β-CDs (E) at pH 3.5 (●), pH 5.5 (○), pH 6.5 (■), pH 7.0 (□) and pH 8.5 (♦). Values represent means of triplicate determination.

756

757

758

759

760

761
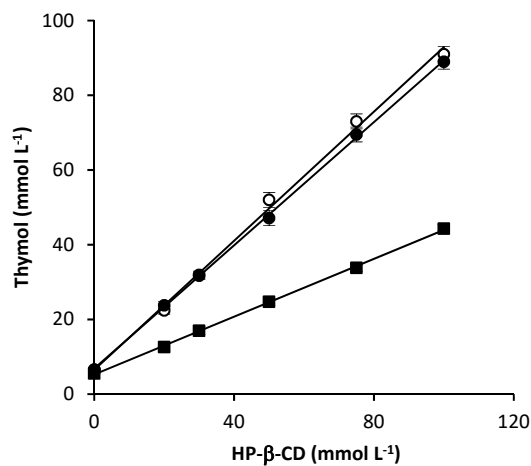
762 Figure 2. Phase solubility diagrams of thymol with HP-β-CD a pH 7.0 using the solubility

763 method (■), the microwave method 24h MWI (○) and 48h MWI (●). Values represent

764 means of triplicate determination.

765

766

767

768

769

770

771

772

773

774

775
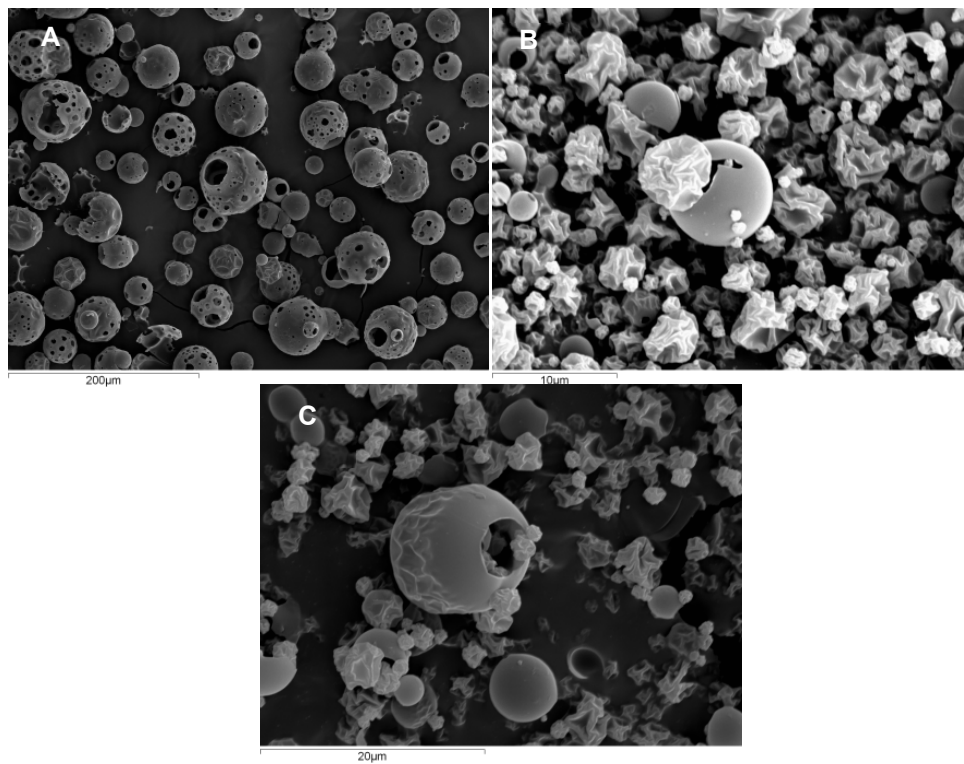
776

Figure 3. Microphotographs of HP-β-CDs (A), MWI method complexes (B) and solubility method complexes (C).

798

799

800

801

802

803

804
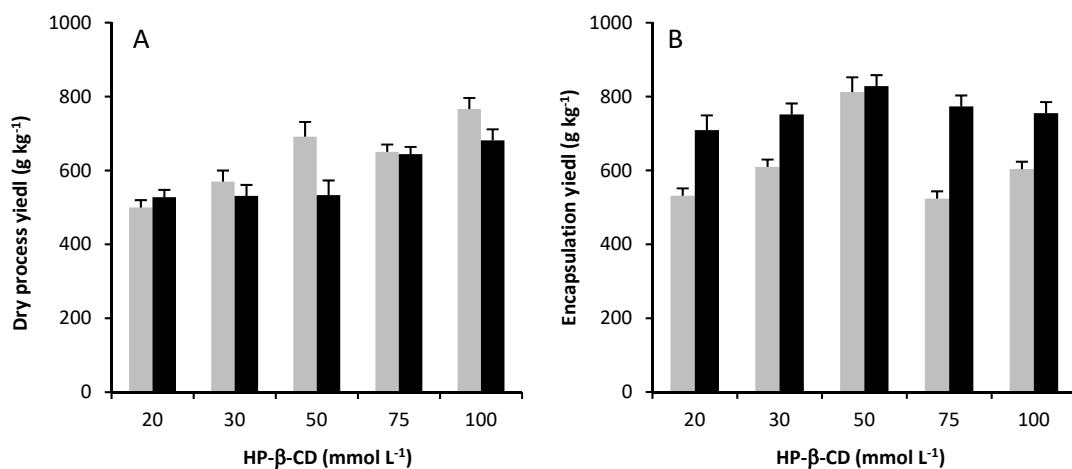
805 Figure 4: Drying process yield (A) (g kg^{-1}) and encapsulation yield of thymol (B) (g kg^{-}

806 ^{1}) of HP-β-CDs-thymol complexes prepared by solubility method (grey bars) and MWI

807 method (black bars). Values represent means of triplicate determination.

808

809

810

811

812

813

814

815

816

817

818

819
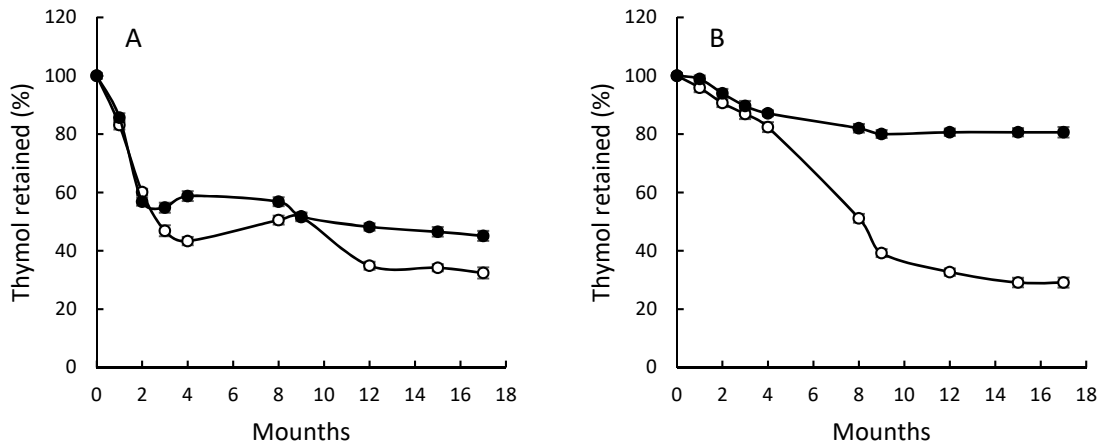
Figure 5. Evolution of thymol retained in solid complexes during 17 months of the storage at 4 ºC (○) and 25ºC (●). Complexes prepared by solubility method (A) and MWI method (B).Values represent means of triplicate determination.

842

843

844

845

846

847

848

849

850
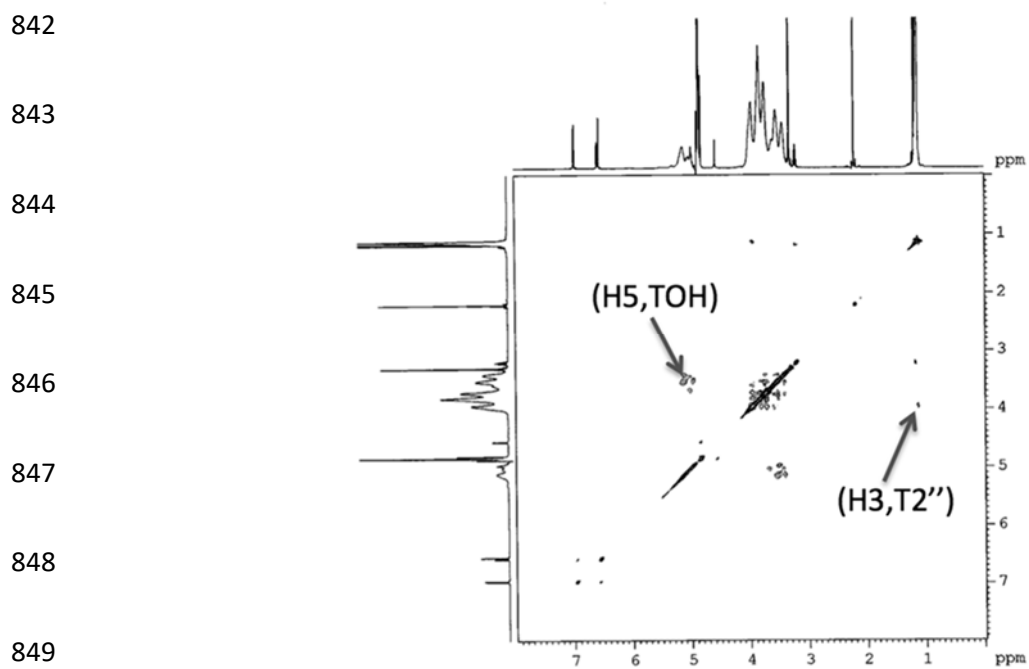
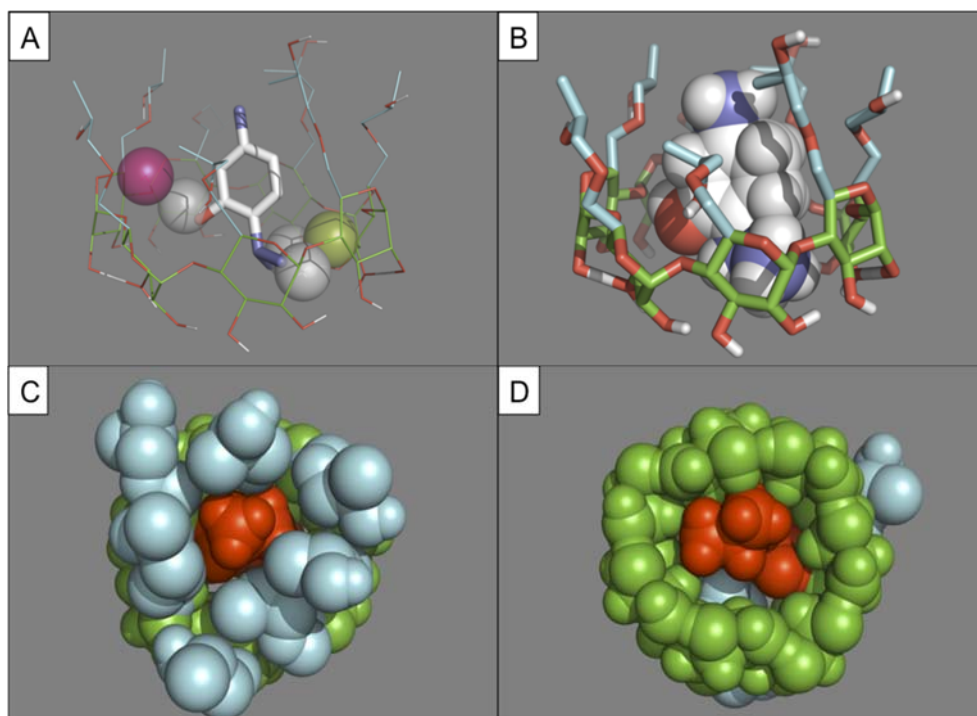851 Figure 6. Evolution ROESY spectrum of HP-β-CDs-thymol complex in D_2O.

852

853

854

855

856

857

858

859

860

861

862

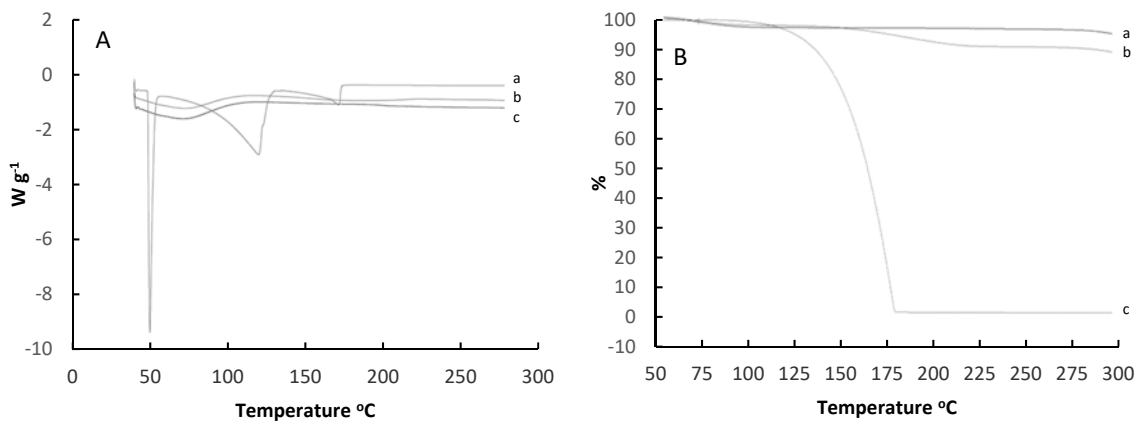Figure 7: 3D perspectives of thymol and HP-β-CDs complexes obtained by molecular docking.

884

885

886

887

888

889

890

891 Figure 8: (A): DSC curves of a) thymol (pink); b) MWI HP-β-CDs-thymol (red); c) HP-

892 β-CDs (green); (B): TG curves of a) HP-β-CDs (green); b) MWI HP-β-CDs-thymol
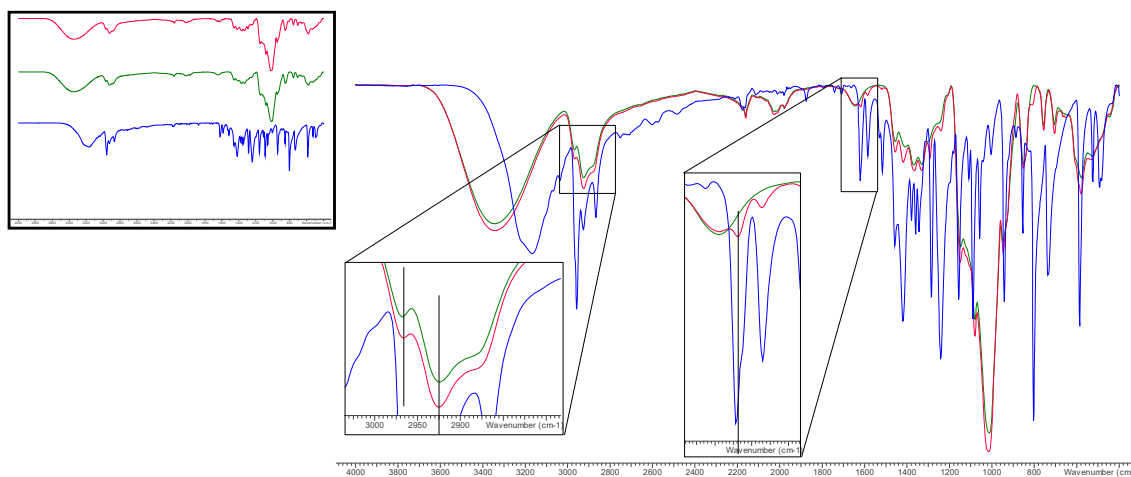
893 (pink); c) thymol (blue).

894

895

896

897

898

899

900

901

902

Figure 9: Inset: FTIR spectra of HP-β-CDs (green), HP-β-CDs-thymol (red) and thymol (blue). Stacked FTIR spectra of HP-β-CDs (green), HP-β-CDs-thymol (red) and thymol (blue). Vertical lines are indicating the maximum of HP-β-CDs-thymol curve.